Published in final edited form as:
Free Radic Biol Med. 2013 August ; 0: 370–383. doi:10.1016/j.freeradbiomed.2013.04.021.

Compartmentalized oxidative stress in dopaminergic cell death induced by pesticides and complex I inhibitors: Distinct roles of superoxide anion and superoxide dismutases

Humberto Rodriguez-Rocha[1,2], **Aracely Garcia-Garcia**[1,2], **Chillian Pickett**[1,2], **Li Sumin**[1,2], **Jocelyn Jones**[4], **Han Chen**[3], **Brian Webb**[5], **Jae Choi**[5], **You Zhou**[1,2,3], **Matthew C. Zimmerman**[1,4], and **Rodrigo Franco**[1,2,✉]

[1]Redox Biology Center, University of Nebraska-Lincoln, Lincoln, NE 68583-0905

[2]School of Veterinary Medicine and Biomedical Sciences, University of Nebraska-Lincoln, Lincoln, NE 68583-0905

[3]Center for Biotechnology, University of Nebraska-Lincoln, Lincoln, NE 68583-0905

[4]Department of Cellular and Integrative Physiology, University of Nebraska Medical Center, Omaha, NE 68198-5850

[5]Thermo Scientific, Research and Development, Rockford IL 61105

Abstract

The loss of dopaminergic neurons induced by the parkinsonian toxins paraquat, rotenone and 1-methyl-4-phenylpyridinium (MPP^+) is associated with oxidative stress. However, controversial reports exist regarding the source/compartmentalization of reactive oxygen species (ROS) generation and its exact role in cell death. We aimed to determine in detail the role of superoxide anion ($O_2^{\bullet-}$), oxidative stress and their subcellular compartmentalization in dopaminergic cell death induced by parkinsonian toxins. Oxidative stress and ROS formation was determined in the cytosol, intermembrane (IMS) and mitochondrial matrix compartments, using dihydroethidine derivatives, the redox sensor roGFP, as well as electron paramagnetic resonance spectroscopy. Paraquat induced an increase in ROS and oxidative stress in both the cytosol and mitochondrial matrix prior to cell death. MPP^+ and rotenone primarily induced an increase in ROS and oxidative stress in the mitochondrial matrix. No oxidative stress was detected at the level of the IMS. In contrast to previous studies, overexpression of manganese superoxide dismutase (MnSOD) or copper/zinc SOD (CuZnSOD) had no effect on ROS steady state levels, lipid peroxidation, loss of mitochondrial membrane potential ($\Delta\Psi m$) and dopaminergic cell death induced by MPP^+ or rotenone. In contrast, paraquat-induced oxidative stress and cell death were selectively reduced by MnSOD overexpression, but not by CuZnSOD or manganese-porphyrins. However, MnSOD also

✉Rodrigo Franco. Redox Biology Center and School of Veterinary Medicine and Biomedical Sciences. 114 VBS 0905. University of Nebraska-Lincoln, Lincoln, NE 68583. Tel: 402-472-8547. Fax: 402-472-9690. rfrancocruz2@unl.edu.

failed to prevent ΔΨm loss. Finally, paraquat, but not MPP^+ or rotenone, induced the transcriptional activation the redox-sensitive antioxidant response elements (ARE) and nuclear factor kappa-B (NF-κB). These results demonstrate a selective role of mitochondrial $O_2^{\bullet-}$ in dopaminergic cell death induced by paraquat, and show that toxicity induced by the complex I inhibitors rotenone and MPP^+ does not depend directly on mitochondrial $O_2^{\bullet-}$ formation.

Keywords

Paraquat; MPP+; rotenone; roGFP; SOD; MnSOD; CuZnSOD; porphyrins; pesticides; environmental; Parkinson's disease

INTRODUCTION

Parkinson's disease (PD) is characterized by the loss of dopaminergic neurons in the *substantia nigra pars compacta* (SNpc) [1]. Post-mortem PD brains have elevated levels of oxidative DNA damage, proteins, and lipids [2–4] supporting a role for oxidative stress in dopaminergic cell loss. However, the molecular events and mechanisms involved remain unknown. Over 90% of the cases occur most commonly in a sporadic (idiopathic) with a pathogenesis likely linked to environmental causes. [5–6].

A dysfunction in the electron transport chain (ETC) has been found in PD brains. Thus, inhibitors of complex I activity are well accepted toxicological models to understand dopaminergic cell death pathways [7]. Recent epidemiological data also suggests a link between the exposure to environmental toxicants such as paraquat and rotenone and an increased risk in developing PD [8]. Dopaminergic cell death induced by parkinsonian toxins has been reported to be tightly linked to the generation of ROS, primarily $O_2^{\bullet-}$ formation. However, contradictory results exist regarding the role of oxidative stress in dopaminergic cell death induced by these toxins. For example, MPP^+/MPTP toxicity has been reported to be inhibited by SOD mimetics [9–10], and overexpression of CuZnSOD [11–12] and MnSOD [13], while MnSOD or CuZnSOD deficiency increases its toxicity [14–15]. In contrast, several studies also show that MPP^+/MPTP toxicity is mediated, at least in part, by a mechanism independent from inhibition of complex I [16] and the generation of ROS [17–23]. Similar conflicting results have been found with respect to the role of complex I inhibition and ROS formation in rotenone-induced toxicity [16–17, 22, 24–26]. Dopaminergic cell death induced by paraquat is largely ascribed to the generation of ROS and oxidative stress [27]. However, while some studies demonstrate that mitochondria are the primary site of ROS formation upon paraquat exposure [28–30], other reports suggest that the cytoplasm is where ROS are primarily generated [31–32].

Based on the controversies summarized above, we aimed to determine the role of superoxide anion ($O_2^{\bullet-}$), oxidative stress, and its compartmentalization in dopaminergic cell death induced by the parkinsonian toxins. The results presented here clearly distinguish, for the first time, a selective role of mitochondrial $O_2^{\bullet-}$ in dopaminergic cell death induced by paraquat, and show that toxicity induced by the complex I inhibitors rotenone and MPP^+ does not depend directly on mitochondrial $O_2^{\bullet-}$ formation.

MATERIALS AND METHODS

Cell Culture and treatments

Human dopaminergic neuroblastoma cells (SK-N-SH) and human IMR-32 neuroblastoma cells (ATCC; Manassas, VA, USA) were cultured as indicated by the provider. Cell culture reagents were obtained from Thermo Scientific/Hyclone (Logan UT) or Invitrogen/GIBCO (Carlsbad, CA). Paraquat (1,1′-Dimethyl-4,4′-bipyridinium dichloride), 1-methyl-4-phenylpyridinium iodide (MPP^+) and rotenone were obtained from SIGMA/Aldrich (St. Louis, MO).

Recombinant Adenoviral vectors

Replication-deficient recombinant adenoviruses (Ad5CMV-MnSOD and Ad5CMV-CuZnSOD were used to overexpress MnSOD or CuZnSOD and have been described previously [33–34]. Adenovirus containing only the CMV promoter (AdEmpty) was used as negative control. Adenoviruses were amplified and tittered in HEK293T cells as described previously [35–36]. Cells were infected with adenoviral vectors at a multiplicity of infection (MOI) of 0.15 and treated with experimental conditions at 24 hours (h) post-infection.

Cytotoxicity assay (mitochondrial activity)

Mitochondrial activity was assessed as a marker of cytotoxicity by measuring the conversion of the tetrazolium salt MTT to formazan as described in [36]. 7,500 cells per well (96-well format) were initially plated. The amount of formazan dye produced is directly proportional to the number of metabolically active cells and indicates the reducing potential of the cell.

Cell death (loss of plasma membrane integrity) determination

Loss of cell viability was determined using flow cytometry (FACS, Fluorescence Activated Cell Sorting) by measuring either propidium iodide (PI, 1 μg/ml) or Sytox Blue uptake (5 nM) (Invitrogen/Molecular Probes) as markers for plasma membrane integrity loss. PI was detected using FL-3 (488 nm excitation, 695/40 nm emission) or L2-4 (561 nm ex, 615/25 nm em), and Sytox Blue (407 nm ex, 450/50 nm em) in a BDFACSort (Cytek-DxP-10 upgrade). Data were analyzed using FlowJo 7.6.5 software. When indicated, cells were pretreated with Mn(III)tetrakis(4-benzoic acid)porphyrin chloride (MnTBAP) or Mn(III)tetrakis(1-methyl-4-pyridyl)porphyrin tetratosylate hydroxide (MnTMPyP). MnTBAP was resuspended in 0.1 mM NaOH. Alternatively, cell death was assessed using a Calcein retention assay which measures both the number of cells attached and the integrity of the plasma membrane. Cells were incubated with 1 μg/ml Calcein-AM for 30 min. Then cells were washed and analyzed at 485 nm ex and 520 nm em in a FLUOstar OPTIMA plate reader (BMG Labtech, Cary, NC).

ROS formation and oxidative stress in mitochondrial and cytosolic compartments

ROS production was determined using dihydroethidine (DHE) (Invitrogen/Molecular Probes), which after its oxidization to ethidium intercalates within the DNA and exhibits bright red fluorescence. ROS production in the mitochondria was assessed using Mitosox Red (Invitrogen/Molecular Probes), a derivative of DHE with a cationic

triphenylphosphonium substituent responsible for the electrophoretic uptake into actively respiring mitochondria. Cells were incubated with DHE or Mitosox (5 μM) and their oxidation was monitored by flow cytometry using FL-2 (488 nm ex, 585/42 nm em) or L3-2 (407 nm ex, 545/30 nm emission).

Alterations in the redox state of both cytosol and mitochondrial compartments were monitored using the reduction-oxidation sensitive green fluorescent protein (roGFP). roGFP sensor allows the noninvasive monitoring of intracellular thiol-disulfide equilibrium, whose fluorescence is determined by the oxidation state of two cysteines introduced into the structure of the GFP. Expression vectors encoding roGFP1 and roGFP1 with a mitochondrial targeting sequence (Mito-roGFP containing the pyruvate dehydrogenase E1α subunit leader sequence) were obtained from Dr. Remington's lab (University of Oregon, Eugene, OR) [37]. roGFP was targeted to the intermembrane space (IMS) using the IMS-targeting signal at the N-terminal amino acid sequence (residues 10–57) from Smac/DIABLO (RSVCSLFRYRQRFPVLANSKKRCFSELIKPWHKTVLTGFGMTLCAVPI), an approach that has been shown to target functional fluorescent proteins into the mitochondrial intermembrane space. This sequence was kindly provided by Dr. Takeaki Ozawa (Department of Chemistry, University of Tokyo, Tokyo, Japan) [38]. All plasmids were linearized with *Nde I* and transfected into SK-N-SH cells using FuGENE HD (Promega, Madison, WI, USA). Stable overexpressing cells were selected in complete medium containing 0.3 mg/ml G418 and GFP positive cell sorting was carried out in a BD FACSAria cell sorter (BD Biosciences, San Jose, CA). roGFP oxidation results in reciprocal changes in emission intensity when excited at two different wavelengths. Changes in roGFP fluorescence were monitored at the single cell level by flow cytometry using ratiometric analysis of roGFP by its dual excitation at 407 and 488 nm and 530 nm emission.

Protein extraction and western immunobloting

Western-immunoblots were performed as explained in [36]. Blots were incubated with the corresponding primary antibody overnight (1:1000): MnSOD (Abnova, Taipei, Taiwan); CuZnSOD, VDAC and GAPDH (Cell Signaling, Danvers, MA). Blots were re-probed to verify equal protein loading.

Confocal microscopy

Cells were grown on glass bottom dishes (MatTek, Ashland, MA) coated with poly-D-lysine (0.1 mg/ml) and incubated with MitoTracker Deep Red (500 nM, 15 min) to label mitochondria. MitoTracker was removed after incubation and live cells were analyzed using an inverted (Olympus IX 81) confocal microscope. (Mito-/IMS-)roGFP was visualized using 488 nm ex laser wavelength and 505–525 nm em. MitoTracker Deep Red was analyzed using 633 nm ex and 660IF emission filter.

Isolation of mitochondrial and cytosolic fractions

Mitochondrial fraction was isolated as described in [39]. Briefly, cells were harvested by trypsinization and then resuspended and homogenized in ice-cold isolation buffer-1 (IB-1: 225 mM mannitol, 75 mM sucrose and 30 mM Tris.Cl, pH 7.4, 0.1 mM EGTA), using a teflon-glass homogenizer. Samples were centrifuged twice (600 g) to remove the nuclei,

debris and the supernatant was centrifuged again (7,000 g). Supernatants containing plasma membrane, lisosomes, microsomes and cytosol fractions were collected for further analysis. Pellets were washed twice in IB-2 (225 mM mannitol, 75 mM sucrose and 30 mM Tris-HCl) and centrifuged at 7,000 g and 10,000 g. Crude mitochondria pellet was resuspended in 2 ml of mitochondria resuspension buffer (MRB: 250 mM mannitol, 5 mM HEPES, pH 7.4 and 0.5 mM EGTA) and then layered on top of percoll solution (225 mM mannitol, 25 mM sucrose, 1 mM EGTA and 30% percoll, v/v) in polypropylene tubes for SW41 Ti rotor (Beckman). Additional MRB was layered on top of mitochondria. After centrifugation (95,000 g), a band containing purified mitochondria was isolated and diluted 10 times in MRB. After centrifugation (6300 g × 10 min, 4°C), mitochondria pellet was gently resuspended in MRB.

Transmission electron microscopy (TEM)

Cells were fixed with 2% glutaraldehyde in 0.2 M HEPES (pH 7.4) for 2 h at room temperature. Fixed cells were collected and post-fixed with 1% OsO_4 in 0.2 M 4-(2-hydroxyethyl)-1-piperazineethanesulfonic acid (HEPES), and stained in 2% uranyl acetate [40]. The pellets were dehydrated through a graduated ethanol series and embedded in Epon 812 (Electron Microscopic Sciences, Fort Washington, PA) for sectioning and observed under a transmission electron microscope (Hitachi H7500). A series of ultrastructural images were collected with a bottom-mount digital camera for the analysis of mitochondria.

Electron Paramagnetic Resonance (EPR) Spectroscopy

After treatment, cells were loaded with the $O_2^{\bullet -}$-sensitive cyclic hydroxylamine cell permeable spin probe CMH (1-hydroxy-3-methoxycarbonyl-2,2,5,5-tetramethylpyrrolidine) (200 μM; 30–60 min) in EPR buffer (Krebs-HEPES buffer pH 7.4 consisting of [in mM]: 99 NaCl, 4.69 KCl, 2.5 $CaCl_2$, 1.2 $MgSO_4$, 25 $NaHCO_3$, 1.03 KH_2PO_4, 5.6 D-glucose, 20 HEPES and supplemented with the metal chelators DETC [5 μM] and deferoxamine [25 μM pH 7.4]). After incubation, cells were collected and placed into the Bruker e-scan EPR spectrometer (Billerica, MA). The following EPR settings were used for all experiments: field sweep width, 60.0 G; microwave frequency, 9.75 kHz; microwave power, 21.90 mW; modulation amplitude, 2.37 G; conversion time, 10.24 ms; time constant, 40.96 ms. Levels of $O_2^{\bullet -}$ were normalized to the number of cells in each sample.

Luciferase reporter assays

The ARE, NFkB, XRE-*Gaussia* and -*Cypridina* Luc reporter plasmids were constructed by cloning each response element plus minimal promoter into Pierce promoterless pMCS-Luciferase Reporter Plasmids (Part No. 16146, Part No. 16149, Part No. 16152). Three plasmids (ARE-*Gaussia*, ,NFkB-*Cypridina*, and CMV-Red Firefly) were transfected into 1.0 × 10^5 cells for 24 hours using Pierce TurboFect Transfection Reagent. At 24 hours post-transfection, cells were treated with the indicated neurotoxins for 4 to 5 hours to activate the signal transduction pathway. The media (*Gaussia* activity) was carefully collected for activity measurement. Then, the cells were lysed with Pierce Luciferase Cell Lysis Buffer. Cypridina and Red Firefly activities in lysate were determined using the luciferase dual assay reagents (Part No. 16181). *Gaussia* and *Cypridina* activities were normalized by Red

Firefly activities. Bioluminescence signals (RLUs) were detected using a Thermo Scientific Varioskan Flash Luminometer equipped with reagent injectors (signal integration time = 1 sec) and filter sets in the ranges of 425 to 525nm for *Cypridina* Luc and 615nm LP for Red Firefly Luc.

Lipid peroxidation

Lipid peroxidation was determined using the ratiometric probe BODIPY C11 (Invitrogen/Molecular Probes), whose fluorescence emission at 590 nm (bright red fluorescence) decreases in response to oxidation with a concomitant increase in bright green fluorescence (530 em) [41–42]. Cells were incubated for 30 min prior to FACS analysis with BODIPY C11 (2.5 μM) and their oxidation was monitored by flow cytometry using FL-1 (488 nm ex, 530/30 nm em) and L2-3 (561 nm ex, 590/20 nm). Results were analyzed ratiometrically 530/590 nm em normalized with control values.

Mitochondrial membrane potential ΔΨm

Alterations in ΔΨm were evaluated using tetramethylrhodamine (TMRM, Invitrogen/Molecular Probes) whose accumulation in the mitochondria is driven by the ΔΨm. Cells are incubated with 50nM TMRM 15 min prior to FACS analysis and TMRM fluorescence is measured using 561 nm ex, and 580/20 nm em.

Statistical analysis

Experiment replicas were independent and performed on separate days. Collected data were analyzed according to statistical criteria by using paired or unpaired t-test, one-way ANOVA or two-way ANOVA, and the appropriate parametric or non-parametric normality post-test using SIGMA-PLOT/STAT package. A probability value of $p<0.05$ was considered as statistically significant. Data were plotted as mean values of at least three independent experiments ± standard error of the mean (SE) using the same statistical package for data analysis. Flow cytometry plots and western blots presented are representative of at least three independent experiments.

RESULTS

Mitochondrial $O_2^{\bullet-}$ formation in response to parkinsonian toxins

Paraquat toxicity is largely ascribed to the generation of $O_2^{\bullet-}$. However, while some studies demonstrate that mitochondria are the primary source of ROS formation upon paraquat exposure [28–30, 43–44], other reports suggest that oxidative stress mainly happens in the cytosol [31–32]. We first evaluated whether paraquat induces ROS production, specifically in the cytosol or mitochondria using the dihydroethidium derivatives DHE and MitoSOX, respectively. Figure 1A–B and E demonstrate that paraquat induces both cytosolic and mitochondrial ROS formation, which parallels cell death. MPP^+ and rotenone treatment also resulted in an increase in cell death and ROS production in a time-dependent manner, which was primarily restricted to the mitochondrial compartment (Figure 1C–D and E). These results demonstrate that while these parkinsonian neurotoxins induce to a similar extent mitochondrial ROS production, paraquat induces major cytosolic ROS accumulation.

SODs are metalloenzymes that catalyze the conversion of $O_2^{\bullet -}$ to hydrogen peroxide (H_2O_2). CuZnSOD has primarily cytoplasmic localization, although it can also be found in the peroxisomes, lysosomes, nucleus, and mitochondrial intermembrane space (IMS), while MnSOD is located in the mitochondrial matrix [45]. We overexpressed MnSOD and CuZnSOD using adenoviral vectors (Figure 2A) and determined their effect on ROS formation induced by paraquat, MPP^+ or rotenone. MnSOD prevents the increase in mitochondrial ROS steady state levels induced by paraquat, while CuZnSOD had no effect on oxidative stress (Figure 2B). In contrast, neither MnSOD nor CuZnSOD overexpression prevented the increase in ROS levels induced by complex I inhibitors (Figure 2C). Paraquat, MPP^+ and rotenone significantly altered mitochondrial morphology assessed by electron microscopy including swelling, matrix thinning and cristea breakdown/disruption (Figure 2D). These results demonstrate that although paraquat, MPP^+ and rotenone act as mitochondrial toxins and induce mitochondrial oxidative damage, only MnSOD is able to reduce ROS accumulation induced by paraquat.

Effect of overexpression of SODs on dopaminergic cell death induced by parkinsonian toxins

We next evaluated the effect of SOD overexpression on dopaminergic cell death induced by paraquat- MPP^+- and rotenone by flow cytometry analyzing both changes in PI staining and cell shrinkage (a marker for apoptosis) (Figure 3A). Parkinsonian neurotoxins induced a decrease in the population of PI negative cells with normal cell size (see %s in Figure 3A). MnSOD but not CuZnSOD overexpression significantly increased cell survival in the presence of paraquat (Figure 3B). Similar results were observed when mitochondrial activity was determined by MTT assay (Figure 3C). No additive effect was observed by co-expression of both MnSOD and CuZnSOD. In contrast to previous studies [11–15], overexpression of neither CuZnSOD nor MnSOD decreased MPP^+- or rotenone-induced cell death (Figure 3D). Manganese-porphyrins, MnTBAP and MnTMPyP, failed to reduce dopaminergic cell death induced by paraquat, and mitochondrial ROS detection (Figure 3E, and supplementary Figure 5C). These results demonstrate that while paraquat-induced cell death is directly dependent on the generation of $O_2^{\bullet -}$ in the mitochondria, the mechanism by which MPP^+ and rotenone induce toxicity might involve additional events besides mitochondrial $O_2^{\bullet -}$ formation.

Alterations in the redox state of cytosol and mitochondria compartments in response to parkinsonian neurotoxins

To study more in detail the alterations in the redox state induced by paraquat, MPP+ or rotenone, we use the redox sensor roGFP. Cells were stably transfected with roGFP, Mito-roGFP and IMS-roGFP. The expression, localization and functionality of the redox sensors were determined by confocal microscopy and flow cytometry. While roGFP was distributed throughout the cell, Mito-roGFP (Figure 4A) and IMS-roGFP (Supplementary Figure 2A) colocalized with mitochondria staining. Ratiometric analysis at 407/488 nm ex - 530 nm em demonstrated the functionality and sensitivity of these cells to oxidizing (H_2O_2) and reducing conditions (dithiothreitol, DTT) (Supplementary Figure 1). To determine alterations in the cellular redox balance occurring prior to cell death, we only analyzed viable cells that have not lost the plasma membrane integrity (*PI- cells depicted in the*

histogram of Figure 4B). Paraquat and MPP^+ significantly increased oxidative stress in the mitochondrial matrix at 24 h (Figure 4B, *left panels*). At 48 h, there was a dose-response increase in both mitochondrial matrix and cytoplasmic oxidative stress (Figure 4B, *right panels*) upon paraquat exposure. Neither paraquat nor MPP^+ increased oxidative stress in the intermembrane space (IMS-rogfp, Supplementary Figure 2B–C). Rotenone failed to induce alterations in the cellular redox state measured by roGFP and Mito-roGFP. However a slight increase in IMS-roGFP signal was detected (Figure 4B, and Supplementary Figure 2C).

When analyzing the relationship between oxidative stress and cell death we observed that there was a strong correlation between both oxidative stress in the cytosolic and mitochondrial compartments, and cell death induced by paraquat (Figure 5A–B). In contrast, MPP^+ toxicity was only associated with a slight increase in mitochondrial oxidative stress (Figure 5B). Similar to the observations obtained using dihydroethidium derivatives, overexpression of MnSOD but not CuZnSOD significantly reduced mitochondrial oxidative stress in paraquat treated cells (Figure 5C), while overexpression of MnSOD had no effect on mitochondrial oxidative stress induced by MPP^+ (Figure 5D). These results demonstrate that paraquat induces an early increase in oxidative stress in the mitochondrial matrix associated to $O_2^{\bullet -}$ formation, followed by subsequent oxidative stress in the cytosol. Furthermore, they confirmed that mitochondrial oxidative stress induced by MPP^+ cannot be prevented by overexpression of MnSOD, suggesting that alterations in the redox balance induced by MPP^+ might involve a distinct source of oxidative stress besides $O_2^{\bullet -}$. It is important to mention that the differences in the kinetic responses between roGFP, Mito-roGFP and IMS-roGFP cells to distinct concentrations of paraquat, MPP^+ and/or rotenone cannot be ascribed to intrinsic differences between the stable cell lines overexpressing the roGFP sensors, as their sensitivity to cell death was similar (Figure 5E–F, and Supplementary Figure 3)

Detection of superoxide anion and free radical formation induced by parkinsonian toxins using EPR

Although EPR has low sensitivity relative to the reactivity to most free radicals, it is considered the primary and most unambiguous technique for detection of free radicals, which makes it an excellent approach to study oxidative stress in response to parkinsonian toxins. Oxidation of the spin probe CMH was used to detect free radical-formation. CMH oxidation-dependent EPR signal was increased by exposure to parkinsonian toxins in a time- and dose-dependent manner (Figure 6A and Supplementary Figure 4A–B). Overexpression of MnSOD but not CuZnSOD significantly decreased CMH oxidation induced by paraquat (Figure 6B and C). In contrast, SOD overexpression had no effect on oxidative stress induced by MPP^+ or rotenone (Figure 6C and Supplementary Figure 4C–D).

Activation of ARE- and NF-κB-driven reporters and lipid peroxidation by parkinsonian neurotoxins

Oxidative stress activates the transcription of a variety of antioxidant genes through cis-acting sequences known as antioxidant response elements (ARE). Similarly, oxidative stress has been largely demonstrated to activate NF-κB-dependent transcription of pro-survival genes [46]. We next determined the activation of both ARE- and NF-κB-driven reporters

(Figure 6D) in response to parkinsonian mimetics as a measurement of oxidative stress and cellular antioxidant response. Figure 6D shows that paraquat but not complex I inhibitors, triggered transcriptional activity driven by ARE and NF-κB reporters.

Lipids are major targets of ROS and lipid peroxidation is a major consequence of oxidative damage [47]. Thus, we also evaluated the effects of SOD overexpression on lipid peroxidation-induced by parkinsonian mimetics. Figure 6E demonstrates that paraquat-induced lipid peroxidation is higher compared to MPP^+ and rotenone. Regardless, only MnSOD overexpression reduces paraquat induced lipid peroxidation. Overall, these results demonstrate that oxidative stress and cell death induced by paraquat are directly linked to $O_2^{\bullet -}$ formation in the mitochondria, while oxidative stress and cell death associated with complex I inhibition involves additional mechanisms besides mitochondrial $O_2^{\bullet -}$.

Loss of mitochondrial membrane potential (ΔΨm) by paraquat is not prevented by MnSOD

As shown in Figure 2D (electron microscopy), paraquat, MPP^+ and rotenone induce profound alterations in mitochondrial structure, while overexpression of MnSOD prevents the loss of mitochondrial activity-induced by paraquat (Figure 3C). To further study the role of paraquat-induced $O_2^{\bullet -}$ in mitochondrial function we evaluated alterations in ΔΨm induced by paraquat. Figure 7A shows that cell death induced by paraquat, MPP^+ or rotenone is paralleled by a decrease in ΔΨm (*upper left quadrants in contour plots*). A population of viable cells with a decrease in ΔΨm (*lower left quadrants*) was significantly increased in response to MPP^+ and rotenone treatments (Figure 7B), suggesting that ΔΨm loss precedes cell death. Neither overexpression of MnSOD or CuZnSOD had an effect in ΔΨm loss induced by MPP^+ or rotenone. Interestingly, loss of ΔΨm upon paraquat exposure was only detected in the population of dead cells (Figure 7A *upper left quadrants*). MnSOD overexpression decreased cell death induced by paraquat (Figure 7A *upper quadrants*, and Figure 3B). However, it did not alter ΔΨm loss and, as a result, induced an accumulation of viable cells with a decrease in ΔΨm (Figure 7A *lower left quadrants, and* Figure 7B). These results demonstrate that depolarization of ΔΨm in response to paraquat is independent from mitochondrial $O_2^{\bullet -}$ formation.

DISCUSION

Controversial reports exist regarding the source/compartmentalization of ROS generation and its exact role in dopaminergic cell death induced by complex I inhibitors and pesticides. We have done a thorough analysis to determine the role of $O_2^{\bullet -}$, oxidative stress and its compartmentalization in dopaminergic cell death induced by parkinsonian toxins. We found that paraquat induced an early increase in mitochondrial $O_2^{\bullet -}$ and oxidative stress, which was followed by further oxidative stress in the cytosol. Oxidative stress and cell death were inhibited by overexpression of MnSOD, but not by CuZnSOD or Mn-porphyrins, demonstrating that mitochondrial $O_2^{\bullet -}$ formation is the primary event regulating oxidative stress and cell death induced by paraquat. In contrast, MPP^+- or rotenone- induced toxicity and oxidative stress were insensitive to MnSOD or CuZnSOD overexpression suggesting that additional mechanisms besides $O_2^{\bullet -}$ formation are involved in the toxicity induced by complex I inhibition

MPP^+/MPTP toxicity is ascribed to the inhibition of complex I [48]. Overexpression of CuZnSOD [11–12] or MnSOD [13] has been shown to decrease MPTP toxicity, while MnSOD or CuZnSOD deficiencies increase it [14–15]. In this study, MPP^+-induced toxicity was prevented by neither MnSOD nor CuZnSOD overexpression. The discrepancies might relate to the model system used. Glial cells participate in MPTP and rotenone toxicity as sources of ROS formation and inflammatory responses [49–50]. Thus, the effect of SOD overexpression or deficiency *in vivo* might be ascribed to the regulation of ROS production from glial cells. Our aim was to determine the role of ROS and its compartmentalization specifically in dopaminergic cells, and thus, the use of *in vivo* experimental models or mixed dopaminergic neuronal primary cultures was not suitable for this purpose.

Interestingly, several studies have shown that MPP^+/MPTP toxicity is mediated by mechanisms independent from complex I inhibition [16] and generation of ROS [17–18, 20–23], which might include microtubule depolymerization and energy failure [18, 26]. Similar contradictory results have been found regarding rotenone-induced toxicity [16–17, 22, 24–25, 51]. In our work, overexpression of SODs did not protect against MPP^+ or rotenone toxicity. We cannot rule out a role for oxidative stress in dopaminergic cell death induced by complex I inhibition as the overexpression of SODs had no effect on oxidative stress induced by MPP^+ or rotenone. However, our results strongly argue against a direct role of $O_2^{\bullet -}$ formation. There is a possibility that overexpressed MnSOD fails to scavenge $O_2^{\bullet -}$. However, this is unlikely because MnSOD overexpression inhibited cell death induced by paraquat, which is paralleled by a higher degree of mitochondrial ROS formation and oxidative stress (lipid peroxidation) (See Figure 1B, 5B and 6E).

$O_2^{\bullet -}$ reacts with nitric oxide ($NO^{\bullet}$) to form peroxynitrite ($ONOO^-$) three times faster than $O_2^{\bullet -}$ dismutation by SOD [52] and MnSOD has been reported to be inactivated by tyrosine nitration [53]. Because $NO^{\bullet}$ and $ONOO^-$ participate in MPP^+/MPTP and rotenone toxicity [54–57], $O_2^{\bullet -}$ could mediate its toxic effects by $ONOO^-$ formation. Another possibility is that dismutation of $O_2^{\bullet -}$ by SODs leads to accumulation of H_2O_2. However, when CuZnSOD or MnSOD were overexpressed together with catalase or mitochondria targeted catalase using adenoviral vectors [58], there still was no protection against MPP^+ or rotenone toxicity (data not shown). In addition, high extracellular GSH (25 mM), N-acetyl-cysteine (25 mM) or cell permeable GSH-ester (1 mM) failed to prevent toxicity induced by complex I inhibition (data not shown). These results would suggest that energy failure but not oxidative stress mediates dopaminergic cell death induced by complex I inhibition as previously suggested [17–18, 20–23]. Our next step would be to study and compare independently the role of energy failure *vs* mitochondrial ROS formation in dopaminergic-cell death induced by complex I inhibitors but this requires extensive additional experimental work.

Oxidative stress induced by intracellular dopamine oxidation but not mitochondrial ROS formation has been proposed as a major contributor to MPP^+ toxicity [59]. A protective role for both cytosolic peroxiredoxin 2 (Prx2) and mitochondrial Prx3 against MPP^+/MPTP toxicity has been demonstrated [60–61]. We observed that MPP^+ and rotenone induced toxicity was associated with only a minor, but significant increase in oxidative stress in the cytosol (Figure 4B and 5A). In addition, MPP^+ and rotenone failed to activate redox-

sensitive ARE- or NF-κB reporters (Figure 7). Our results seem to suggest then that oxidative stress induced by inhibition of complex I is primarily restricted to the mitochondrial matrix.

While some studies demonstrate that mitochondria are the primary source of ROS formation upon paraquat exposure [28–30], other reports suggest that the cytoplasm is the major site for ROS generation [31–32]. We demonstrated that paraquat induces an early increase in mitochondrial oxidative stress that precedes the rise in cytoplasmic ROS levels. This was demonstrated by the early increase in Mito-roGFP signal compared to roGFP fluorescence. This difference was not related to alterations in the cellular sensitivity to paraquat by the expression of the redox sensors. Furthermore, the ratiometric nature of (mito-)roGFP analyses rules out differences ascribed to expression levels of roGFP and/or alterations in pH. Paraquat also induced the transcriptional activation of ARE- and NF-κB reporters and lipid peroxidation. Cell death and oxidative stress induced by paraquat was inhibited by MnSOD but not CuZnSOD overexpression demonstrating that mitochondria are the primary source for $O_2^{\bullet -}$ formation. Interestingly, overexpression of MnSOD does not prevent the loss of ΔΨm induced by paraquat suggesting that these event is independent from mitochondrial $O_2^{\bullet -}$. Paraquat redox cycle involves its reduction by cellular levels of NADPH, before becoming oxidized by an electron receptor to produce $O_2^{\bullet -}$ inducing NADPH depletion [43, 62]. A recent study reports that that knockdown of nicotinamide nucleotide transhydrogenase (NNT) involved in mitochondrial NADPH generation induces ΔΨm loss [63]. Thus, we speculate that paraquat-induced ΔΨm depolarization is associated to depletion of NADPH levels and not $O_2^{\bullet -}$ formation.

Metalloporphyrin MnTBAP and MnTMPyP, failed to reduce mitochondrial ROS detection by paraquat, rotenone or MPP+, and protect against toxicity (Supplementary Figure 5C). MnTBAP has been shown to decrease dopaminergic apoptosis induced by paraquat *in vivo* [64], but whether this effect is ascribed to a reduction in ROS accumulation in neuronal or glial cells known to contribute to paraquat toxicity was not studied [65–66]. In addition, MnTBAP is an anionic porphyrin with a reduction potential more negative than the potential for oxidation of $O_2^{\bullet -}$. [67–68]. MnTMPyP is fairly prone to accept electrons. However, MnTMPyP might induce toxicity by its association with nucleic acids [67]. Manganese porphyrins also perform cycles of oxidant detoxification by taking electrons from the respiratory chain, and then, reducing oxidants such as $O_2^{\bullet -}$ and $ONOO^-$ [69–70]. Manganese porphyrins also increase oxidative stress and cell death [67, 71–72]. In our study, MnTMPyP increased paraquat toxicity.

To understand the source of ROS formation and their compartmentalization we have used a variety of complementary experimental approaches to: 1) determine ROS formation and oxidative stress (dihydroethidium derivatives); 2) determine alterations in subcellular redox balance/potential (roGFP sensors); 3) free radical formation (EPR); 4) redox signaling (ARE-driven reporters) and oxidative damage (lipid peroxidation). We consider that it is important to summarize and discuss here the limitations ascribed to these assays. Dihydroethidium derivatives are widely used probes for detecting intracellular $O_2^{\bullet -}$. However, direct oxidation of DHE to ethidium (Etd^+) is mediated by ROS such as $ONOO^-$, hydroxyl radical ($OH^\bullet$) and H_2O_2, but not by $O_2^{\bullet -}$. 2OH-Etd^+ formed from the reaction of

DHE with $O_2^{\bullet -}$ can be measured by analytical techniques [73]. Because we aimed to characterize oxidative stress in live cells, this type of analysis could only be done by FACS. Robinson et al. demonstrated that 405 nm ex enhances the fluorescence of 2OH-Etd^+ reducing spectral overlap with Etd^+ [74]. In our experiments, DHE and MitoSOX fluorescence increased primarily at 488 nm ex compared to 407 nm ex (data not shown) suggesting that they mostly detect overall oxidative stress and not only $O_2^{\bullet -}$. In order to detect the formation of free radicals induced by parkinsonian mimetics, we used CMH detection by EPR spectroscopy [75]. However, this approach was recently reported to lack specificity regarding chemical identity of the oxidant/free radical that oxidizes the probe [76]. Regardless, the fact that overexpression of MnSOD did not prevent ROS accumulation (detected by Mitosox and EPR spectroscopy) and oxidative damage (lipid peroxidation) induced by complex I inhibition demonstrates that mitochondria $O_2^{\bullet -}$ is not the primarily mediator of oxidative stress and dopaminergic cell death induced by MPP^+ and rotenone.

To our knowledge, this is the first report characterizing alterations in redox balance of distinct subcellular compartments in response to parkinsonian mimetics using roGFP sensors. A previous study using Mito-roGFP transgenic mice reported increased oxidative stress under basal conditions in dopaminergic neurons of the SNpc [77]. We now demonstrate that alterations in the redox balance induced by MPP^+ are primarily restricted only to the mitochondria. Oxidation of roGFP in response to paraquat was delayed when compared to mito-roGFP suggesting that mitochondrial ROS production precedes cytosolic oxidant production. roGFP oxidation can be promoted by distinct ROS, and roGFP sensors equilibrate with the intracellular thiol-disulfide balance [78]. Thus, alterations in roGFP fluorescence are an indication of oxidative stress but cannot be associated with the detection of a specific ROS. Interestingly, mitochondrial ROS formation induced by rotenone could be detected by Mitosox but not Mito-roGFP. This discrepancy is most likely associated to the nature of the ROS or pro-oxidant condition generated. Supplementary Figure 5A shows that overexpression of SODs does not prevent roGFP oxidation, which might be explained by the increase production of H_2O_2. However, MnSOD does reduce significantly DHE oxidation (Supplementary Figure 5B). Although more experiments are required to clearly identify whether $O_2^{\bullet -}$ or H_2O_2 mediate roGFP oxidation, our observations indicate that an important component of cytosolic oxidative stress is mediated by mitochondrial ROS formation. However, in the cytosol, paraquat most likely also generates ROS. Regardless, only overexpression of MnSOD but not CuZnSOD protects against paraquat toxicity demonstrating that mitochondria are the primary source of ROS upon paraquat exposure.

All together, our results clearly distinguish for the first time a selective role of mitochondrial $O_2^{\bullet -}$ in dopaminergic cell death induced by paraquat, and show that toxicity induced by the complex I inhibitors rotenone and MPP^+ involves additional factors other than mitochondrial $O_2^{\bullet -}$ formation.

Supplementary Material

Refer to Web version on PubMed Central for supplementary material.

Acknowledgments

This work was supported by the National Institutes of Health Grant P20RR17675 Centers of Biomedical Research Excellence (COBRE) (Franco and Zimmerman), R01 HL103942 (Zimmerman), the Research Council Interdisciplinary Grant, and the Life Sciences Grant Program of the University of Nebraska-Lincoln (Franco). We would like to thank Dr. Charles A. Kuszynski, Daniel Shea and Zhi Hong Gill at the Nebraska Center for Virology for their help in the flow cytometry analyses and cell sorting, as well as Terri Fangman at the Morrison Microscopy Core Research Facility for her help in the confocal microscopy analyses.

Abbreviations

ARE	Antioxidant response elements
DHE	dihydroethidium
ETC	electron transport chain
CuZnSOD	copper/zinc SOD
IMS	intermembrane space
MnSOD	manganese SOD
MPP^+	1-methyl-4-phenylpyridinium
$\Delta\Psi m$	mitochondrial membrane potential
MnTBAP	Mn(III)tetrakis(4-benzoic acid)porphyrin chloride
MnTMPyP	Mn(III)tetrakis(1-methyl-4-pyridyl)porphyrin tetratosylate hydroxide
$NO^\bullet$	nitric oxide
NF-κB	nuclear factor kappa-B
PD	Parkinson’s disease
$ONOO^-$	peroxynitrite
PI	propidium iodide
ROS	reactive oxygen species
roGFP	reduction-oxidation sensitive green fluorescence protein
SOD	superoxide dismutase
SNpc	substantia nigra pars compacta
$O_2^{\bullet-}$	superoxide anion

REFERENCES

1. Lees AJ. Unresolved issues relating to the shaking palsy on the celebration of James Parkinson's 250th birthday. Mov Disord. 2007; 22(Suppl 17):S327–S334. [PubMed: 18175393]
2. Alam ZI, Daniel SE, Lees AJ, Marsden DC, Jenner P, Halliwell B. A generalised increase in protein carbonyls in the brain in Parkinson's but not incidental Lewy body disease. J Neurochem. 1997; 69:1326–1329. [PubMed: 9282961]
3. Dexter DT, Carter CJ, Wells FR, Javoy-Agid F, Agid Y, Lees A, Jenner P, Marsden CD. Basal lipid peroxidation in substantia nigra is increased in Parkinson's disease. J Neurochem. 1989; 52:381–389. [PubMed: 2911023]

4. Alam ZI, Jenner A, Daniel SE, Lees AJ, Cairns N, Marsden CD, Jenner P, Halliwell B. Oxidative DNA damage in the parkinsonian brain: an apparent selective increase in 8-hydroxyguanine levels in substantia nigra. J Neurochem. 1997; 69:1196–1203. [PubMed: 9282943]
5. Horowitz MP, Greenamyre JT. Gene-environment interactions in Parkinson's disease: the importance of animal modeling. Clin Pharmacol Ther. 2010; 88:467–474. [PubMed: 20811350]
6. Vance JM, Ali S, Bradley WG, Singer C, Di Monte DA. Gene-environment interactions in Parkinson's disease and other forms of parkinsonism. Neurotoxicology. 2010; 31:598–602. [PubMed: 20430055]
7. Cannon JR, Greenamyre JT. Neurotoxic in vivo models of Parkinson's disease recent advances. Prog Brain Res. 2010; 184:17–33. [PubMed: 20887868]
8. Tanner CM, Kamel F, Ross GW, Hoppin JA, Goldman SM, Korell M, Marras C, Bhudhikanok GS, Kasten M, Chade AR, Comyns K, Richards MB, Meng C, Priestley B, Fernandez HH, Cambi F, Umbach DM, Blair A, Sandler DP, Langston JW. Rotenone, Paraquat and Parkinson's Disease. Environ Health Perspect. 2011
9. Liang LP, Huang J, Fulton R, Day BJ, Patel M. An orally active catalytic metalloporphyrin protects against 1-methyl-4-phenyl-1,2,3,6-tetrahydropyridine neurotoxicity in vivo. J Neurosci. 2007; 27:4326–4333. [PubMed: 17442816]
10. Kaul S, Kanthasamy A, Kitazawa M, Anantharam V, Kanthasamy AG. Caspase-3 dependent proteolytic activation of protein kinase C delta mediates and regulates 1-methyl-4-phenylpyridinium (MPP+)-induced apoptotic cell death in dopaminergic cells: relevance to oxidative stress in dopaminergic degeneration. Eur J Neurosci. 2003; 18:1387–1401. [PubMed: 14511319]
11. Barkats M, Horellou P, Colin P, Millecamps S, Faucon-Biguet N, Mallet J. 1-methyl-4-phenylpyridinium neurotoxicity is attenuated by adenoviral gene transfer of human Cu/Zn superoxide dismutase. J Neurosci Res. 2006; 83:233–242. [PubMed: 16353238]
12. Przedborski S, Kostic V, Jackson-Lewis V, Naini AB, Simonetti S, Fahn S, Carlson E, Epstein CJ, Cadet JL. Transgenic mice with increased Cu/Zn-superoxide dismutase activity are resistant to N-methyl-4-phenyl-1,2,3,6-tetrahydropyridine-induced neurotoxicity. J Neurosci. 1992; 12:1658–1667. [PubMed: 1578260]
13. Klivenyi P, St Clair D, Wermer M, Yen HC, Oberley T, Yang L, Flint Beal M. Manganese superoxide dismutase overexpression attenuates MPTP toxicity. Neurobiol Dis. 1998; 5:253–258. [PubMed: 9848095]
14. Andreassen OA, Ferrante RJ, Dedeoglu A, Albers DW, Klivenyi P, Carlson EJ, Epstein CJ, Beal MF. Mice with a partial deficiency of manganese superoxide dismutase show increased vulnerability to the mitochondrial toxins malonate, 3-nitropropionic acid, and MPTP. Exp Neurol. 2001; 167:189–195. [PubMed: 11161607]
15. Zhang J, Graham DG, Montine TJ, Ho YS. Enhanced N-methyl-4-phenyl-1,2,3,6-tetrahydropyridine toxicity in mice deficient in CuZn-superoxide dismutase or glutathione peroxidase. J Neuropathol Exp Neurol. 2000; 59:53–61. [PubMed: 10744035]
16. Choi WS, Kruse SE, Palmiter RD, Xia Z. Mitochondrial complex I inhibition is not required for dopaminergic neuron death induced by rotenone, MPP+, or paraquat. Proc Natl Acad Sci U S A. 2008; 105:15136–15141. [PubMed: 18812510]
17. Dranka BP, Zielonka J, Kanthasamy AG, Kalyanaraman B. Alterations in bioenergetic function induced by Parkinson's disease mimetic compounds: lack of correlation with superoxide generation. J Neurochem. 2012
18. Cartelli D, Ronchi C, Maggioni MG, Rodighiero S, Giavini E, Cappelletti G. Microtubule dysfunction precedes transport impairment and mitochondria damage in MPP+ -induced neurodegeneration. J Neurochem. 2010; 115:247–258. [PubMed: 20649848]
19. Cappelletti G, Surrey T, Maci R. The parkinsonism producing neurotoxin MPP+ affects microtubule dynamics by acting as a destabilising factor. FEBS Lett. 2005; 579:4781–4786. [PubMed: 16098973]
20. Fonck C, Baudry M. Toxic effects of MPP(+) and MPTP in PC12 cells independent of reactive oxygen species formation. Brain Res. 2001; 905:199–206. [PubMed: 11423095]

21. Lee HS, Park CW, Kim YS. MPP(+) increases the vulnerability to oxidative stress rather than directly mediating oxidative damage in human neuroblastoma cells. Exp Neurol. 2000; 165:164–171. [PubMed: 10964495]
22. Nakamura K, Bindokas VP, Marks JD, Wright DA, Frim DM, Miller RJ, Kang UJ. The selective toxicity of 1-methyl-4-phenylpyridinium to dopaminergic neurons: the role of mitochondrial complex I and reactive oxygen species revisited. Mol Pharmacol. 2000; 58:271–278. [PubMed: 10908294]
23. Sanchez-Ramos JR, Song S, Facca A, Basit A, Epstein CJ. Transgenic murine dopaminergic neurons expressing human Cu/Zn superoxide dismutase exhibit increased density in culture, but no resistance to methylphenylpyridinium-induced degeneration. J Neurochem. 1997; 68:58–67. [PubMed: 8978710]
24. Ahmadi FA, Grammatopoulos TN, Poczobutt AM, Jones SM, Snell LD, Das M, Zawada WM. Dopamine selectively sensitizes dopaminergic neurons to rotenone-induced apoptosis. Neurochem Res. 2008; 33:886–901. [PubMed: 17992568]
25. Yadava N, Nicholls DG. Spare respiratory capacity rather than oxidative stress regulates glutamate excitotoxicity after partial respiratory inhibition of mitochondrial complex I with rotenone. J Neurosci. 2007; 27:7310–7317. [PubMed: 17611283]
26. Choi WS, Palmiter RD, Xia Z. Loss of mitochondrial complex I activity potentiates dopamine neuron death induced by microtubule dysfunction in a Parkinson's disease model. J Cell Biol. 2011; 192:873–882. [PubMed: 21383081]
27. Franco R, Li S, Rodriguez-Rocha H, Burns M, Panayiotidis MI. Molecular mechanisms of pesticide-induced neurotoxicity: Relevance to Parkinson's disease. Chem Biol Interact. 2010; 188:289–300. [PubMed: 20542017]
28. Cocheme HM, Murphy MP. Complex I is the major site of mitochondrial superoxide production by paraquat. J Biol Chem. 2008; 283:1786–1798. [PubMed: 18039652]
29. Castello PR, Drechsel DA, Patel M. Mitochondria are a major source of paraquat-induced reactive oxygen species production in the brain. The Journal of biological chemistry. 2007; 282:14186–14193. [PubMed: 17389593]
30. Drechsel DA, Patel M. Differential contribution of the mitochondrial respiratory chain complexes to reactive oxygen species production by redox cycling agents implicated in parkinsonism. Toxicol Sci. 2009; 112:427–434. [PubMed: 19767442]
31. Cristovao AC, Choi DH, Baltazar G, Beal MF, Kim YS. The role of NADPH oxidase 1-derived reactive oxygen species in paraquat-mediated dopaminergic cell death. Antioxid Redox Signal. 2009; 11:2105–2118. [PubMed: 19450058]
32. Ramachandiran S, Hansen JM, Jones DP, Richardson JR, Miller GW. Divergent mechanisms of paraquat, MPP+, and rotenone toxicity: oxidation of thioredoxin and caspase-3 activation. Toxicol Sci. 2007; 95:163–171. [PubMed: 17018646]
33. Zimmerman MC, Lazartigues E, Lang JA, Sinnayah P, Ahmad IM, Spitz DR, Davisson RL. Superoxide mediates the actions of angiotensin II in the central nervous system. Circ Res. 2002; 91:1038–1045. [PubMed: 12456490]
34. Zwacka RM, Dudus L, Epperly MW, Greenberger JS, Engelhardt JF. Redox gene therapy protects human IB-3 lung epithelial cells against ionizing radiation-induced apoptosis. Hum Gene Ther. 1998; 9:1381–1386. [PubMed: 9650622]
35. Barde I, Salmon P, Trono D. Production and titration of lentiviral vectors. Curr Protoc Neurosci. 2010; Chapter 4(Unit 4):21. [PubMed: 20938923]
36. Rodriguez-Rocha H, Garcia-Garcia A, Zavala-Flores L, Li S, Madayiputhiya N, Franco R. Glutaredoxin 1 protects dopaminergic cells by increased protein glutathionylation in experimental Parkinson's disease. Antioxid Redox Signal. 2012
37. Hanson GT, Aggeler R, Oglesbee D, Cannon M, Capaldi RA, Tsien RY, Remington SJ. Investigating mitochondrial redox potential with redox-sensitive green fluorescent protein indicators. The Journal of biological chemistry. 2004; 279:13044–13053. [PubMed: 14722062]
38. Ozawa T, Natori Y, Sako Y, Kuroiwa H, Kuroiwa T, Umezawa Y. A minimal peptide sequence that targets fluorescent and functional proteins into the mitochondrial intermembrane space. ACS Chem Biol. 2007; 2:176–186. [PubMed: 17348629]

39. Wieckowski MR, Giorgi C, Lebiedzinska M, Duszynski J, Pinton P. Isolation of mitochondria-associated membranes and mitochondria from animal tissues and cells. Nat Protoc. 2009; 4:1582–1590. [PubMed: 19816421]
40. Eskelinen EL. Fine structure of the autophagosome. Methods Mol Biol. 2008; 445:11–28. [PubMed: 18425441]
41. Drummen GP, van Liebergen LC, Op den Kamp JA, Post JA. C11-BODIPY(581/591), an oxidation-sensitive fluorescent lipid peroxidation probe: (micro)spectroscopic characterization and validation of methodology. Free Radic Biol Med. 2002; 33:473–490. [PubMed: 12160930]
42. Pap EH, Drummen GP, Winter VJ, Kooij TW, Rijken P, Wirtz KW, Op den Kamp JA, Hage WJ, Post JA. Ratio-fluorescence microscopy of lipid oxidation in living cells using C11-BODIPY(581/591). FEBS Lett. 1999; 453:278–282. [PubMed: 10405160]
43. Cocheme HM, Murphy MP. Chapter 22 The uptake and interactions of the redox cycler paraquat with mitochondria. Methods Enzymol. 2009; 456:395–417. [PubMed: 19348901]
44. Hinerfeld D, Traini MD, Weinberger RP, Cochran B, Doctrow SR, Harry J, Melov S. Endogenous mitochondrial oxidative stress: neurodegeneration, proteomic analysis, specific respiratory chain defects, and efficacious antioxidant therapy in superoxide dismutase 2 null mice. J Neurochem. 2004; 88:657–667. [PubMed: 14720215]
45. Johnson F, Giulivi C. Superoxide dismutases and their impact upon human health. Mol Aspects Med. 2005; 26:340–352. [PubMed: 16099495]
46. Brigelius-Flohe R, Flohe L. Basic principles and emerging concepts in the redox control of transcription factors. Antioxid Redox Signal. 2011; 15:2335–2381. [PubMed: 21194351]
47. Niki E. Lipid peroxidation: physiological levels and dual biological effects. Free Radic Biol Med. 2009; 47:469–484. [PubMed: 19500666]
48. Cleeter MW, Cooper JM, Schapira AH. Irreversible inhibition of mitochondrial complex I by 1-methyl-4-phenylpyridinium: evidence for free radical involvement. J Neurochem. 1992; 58:786–789. [PubMed: 1729421]
49. Wu DC, Teismann P, Tieu K, Vila M, Jackson-Lewis V, Ischiropoulos H, Przedborski S. NADPH oxidase mediates oxidative stress in the 1-methyl-4-phenyl-1,2,3,6-tetrahydropyridine model of Parkinson's disease. Proc Natl Acad Sci U S A. 2003; 100:6145–6150. [PubMed: 12721370]
50. Gao HM, Liu B, Hong JS. Critical role for microglial NADPH oxidase in rotenone-induced degeneration of dopaminergic neurons. J Neurosci. 2003; 23:6181–6187. [PubMed: 12867501]
51. Richardson JR, Caudle WM, Guillot TS, Watson JL, Nakamaru-Ogiso E, Seo BB, Sherer TB, Greenamyre JT, Yagi T, Matsuno-Yagi A, Miller GW. Obligatory role for complex I inhibition in the dopaminergic neurotoxicity of 1-methyl-4-phenyl-1,2,3,6-tetrahydropyridine (MPTP). Toxicol Sci. 2007; 95:196–204. [PubMed: 17038483]
52. Radi R, Cassina A, Hodara R. Nitric oxide and peroxynitrite interactions with mitochondria. Biol Chem. 2002; 383:401–409. [PubMed: 12033431]
53. Demicheli V, Quijano C, Alvarez B, Radi R. Inactivation and nitration of human superoxide dismutase (SOD) by fluxes of nitric oxide and superoxide. Free Radic Biol Med. 2007; 42:1359–1368. [PubMed: 17395009]
54. Hantraye P, Brouillet E, Ferrante R, Palfi S, Dolan R, Matthews RT, Beal MF. Inhibition of neuronal nitric oxide synthase prevents MPTP-induced parkinsonism in baboons. Nat Med. 1996; 2:1017–1021. [PubMed: 8782460]
55. Liberatore GT, Jackson-Lewis V, Vukosavic S, Mandir AS, Vila M, McAuliffe WG, Dawson VL, Dawson TM, Przedborski S. Inducible nitric oxide synthase stimulates dopaminergic neurodegeneration in the MPTP model of Parkinson disease. Nat Med. 1999; 5:1403–1409. [PubMed: 10581083]
56. LaVoie MJ, Hastings TG. Peroxynitrite- and nitrite-induced oxidation of dopamine: implications for nitric oxide in dopaminergic cell loss. J Neurochem. 1999; 73:2546–2554. [PubMed: 10582617]
57. He Y, Imam SZ, Dong Z, Jankovic J, Ali SF, Appel SH, Le W. Role of nitric oxide in rotenone-induced nigro-striatal injury. J Neurochem. 2003; 86:1338–1345. [PubMed: 12950443]
58. Arita Y, Harkness SH, Kazzaz JA, Koo HC, Joseph A, Melendez JA, Davis JM, Chander A, Li Y. Mitochondrial localization of catalase provides optimal protection from H2O2-induced cell death

in lung epithelial cells. Am J Physiol Lung Cell Mol Physiol. 2006; 290:L978–L986. [PubMed: 16387755]

59. Lotharius J, O'Malley KL. The parkinsonism-inducing drug 1-methyl-4-phenylpyridinium triggers intracellular dopamine oxidation. A novel mechanism of toxicity. J Biol Chem. 2000; 275:38581–38588. [PubMed: 10969076]
60. Qu D, Rashidian J, Mount MP, Aleyasin H, Parsanejad M, Lira A, Haque E, Zhang Y, Callaghan S, Daigle M, Rousseaux MW, Slack RS, Albert PR, Vincent I, Woulfe JM, Park DS. Role of Cdk5-mediated phosphorylation of Prx2 in MPTP toxicity and Parkinson's disease. Neuron. 2007; 55:37–52. [PubMed: 17610816]
61. De Simoni S, Goemaere J, Knoops B. Silencing of peroxiredoxin 3 and peroxiredoxin 5 reveals the role of mitochondrial peroxiredoxins in the protection of human neuroblastoma SH-SY5Y cells toward MPP+ Neurosci Lett. 2008; 433:219–224. [PubMed: 18262354]
62. Suntres ZE. Role of antioxidants in paraquat toxicity. Toxicology. 2002; 180:65–77. [PubMed: 12324200]
63. Yin F, Sancheti H, Cadenas E. Silencing of nicotinamide nucleotide transhydrogenase impairs cellular redox homeostasis and energy metabolism in PC12 cells. Biochim Biophys Acta. 2012; 1817:401–409. [PubMed: 22198343]
64. Peng J, Mao XO, Stevenson FF, Hsu M, Andersen JK. The herbicide paraquat induces dopaminergic nigral apoptosis through sustained activation of the JNK pathway. J Biol Chem. 2004; 279:32626–32632. [PubMed: 15155744]
65. Wu XF, Block ML, Zhang W, Qin L, Wilson B, Zhang WQ, Veronesi B, Hong JS. The role of microglia in paraquat-induced dopaminergic neurotoxicity. Antioxid Redox Signal. 2005; 7:654–661. [PubMed: 15890010]
66. Purisai MG, McCormack AL, Cumine S, Li J, Isla MZ, Di Monte DA. Microglial activation as a priming event leading to paraquat-induced dopaminergic cell degeneration. Neurobiol Dis. 2007; 25:392–400. [PubMed: 17166727]
67. Batinic-Haberle I, Rajic Z, Tovmasyan A, Reboucas JS, Ye X, Leong KW, Dewhirst MW, Vujaskovic Z, Benov L, Spasojevic I. Diverse functions of cationic Mn(III) N-substituted pyridylporphyrins, recognized as SOD mimics. Free Radic Biol Med. 2011; 51:1035–1053. [PubMed: 21616142]
68. Reboucas JS, Spasojevic I, Batinic-Haberle I. Pure manganese(III) 5,10,15,20-tetrakis(4-benzoic acid)porphyrin (MnTBAP) is not a superoxide dismutase mimic in aqueous systems: a case of structure-activity relationship as a watchdog mechanism in experimental therapeutics and biology. J Biol Inorg Chem. 2008; 13:289–302. [PubMed: 18046586]
69. Ferrer-Sueta G, Hannibal L, Batinic-Haberle I, Radi R. Reduction of manganese porphyrins by flavoenzymes and submitochondrial particles: a catalytic cycle for the reduction of peroxynitrite. Free Radic Biol Med. 2006; 41:503–512. [PubMed: 16843831]
70. Valez V, Cassina A, Batinic-Haberle I, Kalyanaraman B, Ferrer-Sueta G, Radi R. Peroxynitrite formation in nitric oxide-exposed submitochondrial particles: detection, oxidative damage and catalytic removal by Mn-porphyrins. Arch Biochem Biophys. 2013; 529:45–54. [PubMed: 23142682]
71. Perez MJ, Cederbaum AI. Antioxidant and pro-oxidant effects of a manganese porphyrin complex against CYP2E1-dependent toxicity. Free Radic Biol Med. 2002; 33:111–127. [PubMed: 12086689]
72. Jaramillo MC, Briehl MM, Crapo JD, Batinic-Haberle I, Tome ME. Manganese porphyrin, MnTE-2-PyP5+, Acts as a pro-oxidant to potentiate glucocorticoid-induced apoptosis in lymphoma cells. Free Radic Biol Med. 2012; 52:1272–1284. [PubMed: 22330065]
73. Zielonka J, Kalyanaraman B. Hydroethidine- and MitoSOX-derived red fluorescence is not a reliable indicator of intracellular superoxide formation: another inconvenient truth. Free Radic Biol Med. 2010; 48:983–1001. [PubMed: 20116425]
74. Robinson KM, Janes MS, Pehar M, Monette JS, Ross MF, Hagen TM, Murphy MP, Beckman JS. Selective fluorescent imaging of superoxide in vivo using ethidium-based probes. Proc Natl Acad Sci U S A. 2006; 103:15038–15043. [PubMed: 17015830]

75. Dikalov SI, Kirilyuk IA, Voinov M, Grigor'ev IA. EPR detection of cellular and mitochondrial superoxide using cyclic hydroxylamines. Free Radic Res. 2011; 45:417–430. [PubMed: 21128732]

76. Ganini D, Canistro D, Jang J, Stadler K, Mason RP, Kadiiska MB. Ceruloplasmin (ferroxidase) oxidizes hydroxylamine probes: Deceptive implications for free radical detection. Free Radic Biol Med. 2012

77. Guzman JN, Sanchez-Padilla J, Wokosin D, Kondapalli J, Ilijic E, Schumacker PT, Surmeier DJ. Oxidant stress evoked by pacemaking in dopaminergic neurons is attenuated by DJ-1. Nature. 2010; 468:696–700. [PubMed: 21068725]

78. Meyer AJ, Dick TP. Fluorescent protein-based redox probes. Antioxid Redox Signal. 2010; 13:621–650. [PubMed: 20088706]

Highlights

- We studied the role of oxidative stress and its compartmentalization in dopaminergic cell death.
- Paraquat-induced oxidative stress and cell death is mediated by mitochondrial superoxide.
- Oxidative stress and cell death induced by MPP^+ and rotenone are not modified by MnSOD or CuZnSOD.
- MnSOD overexpression reduces ROS formation but not $\Delta\Psi m$ loss induced by paraquat.
- Additional mechanisms other than mitochondrial $O_2^{\bullet -}$ are required for MPP+ and rotenone toxicity.

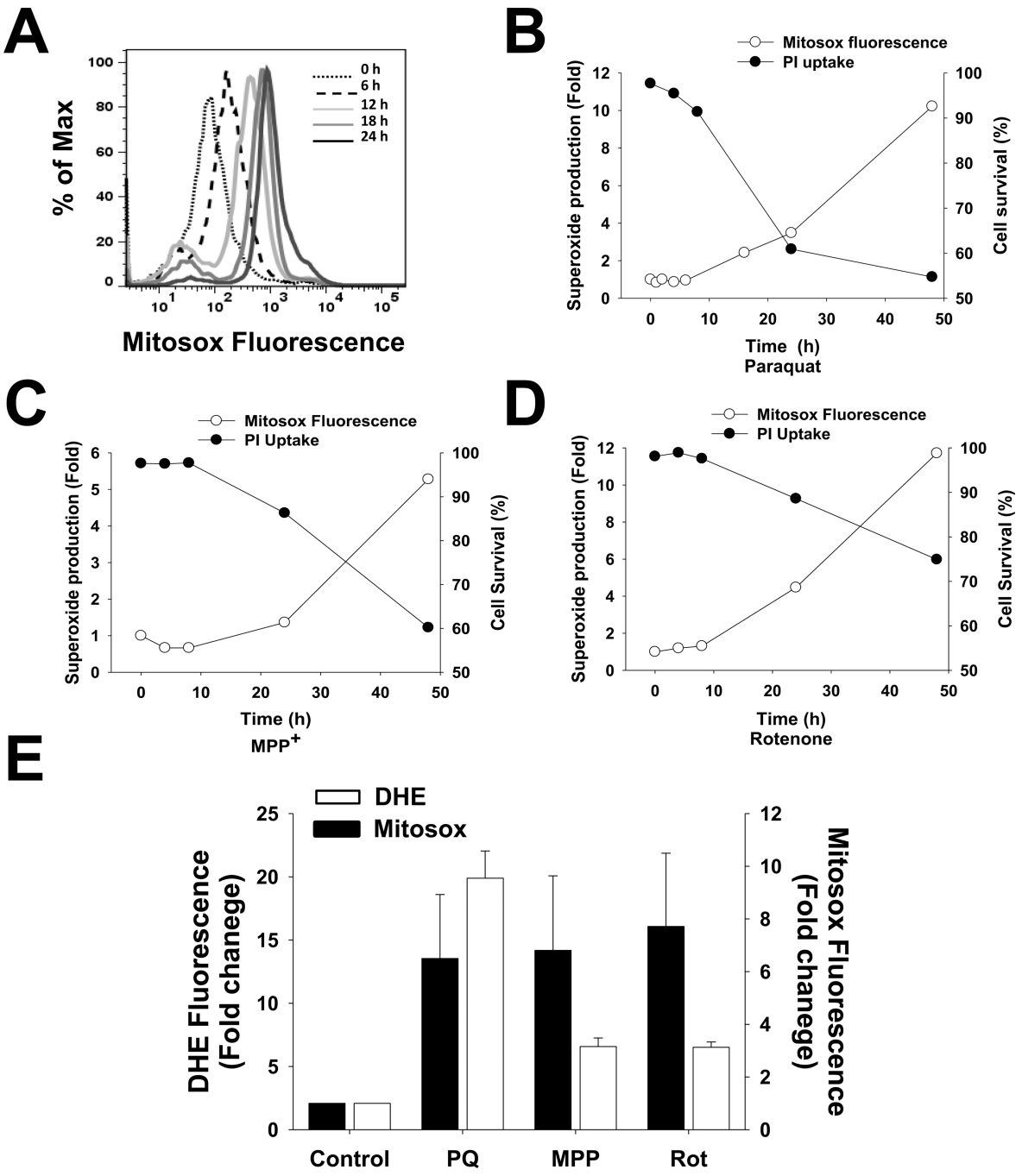

Figure 1. ROS detection using dihydroethidium derivatives

In **A–D**, SK-N-SH cells were treated with 0.5 mM paraquat, 2.5 mM MPP^+ or 4 μM rotenone for the time indicated. Then, cells were stained with Mitosox (mitochondrial $O_2^{\bullet -}$) or propidium iodide (cell death), and analyzed by FACS. Histogram in **A** depicts the changes in the Mitosox mean fluorescence in response to paraquat. In **B–D,** data are expressed as $O_2^{\bullet -}$ production (Mitosox fluorescence) and cell survival (% of cells with low Propipdium iodide staining) normalized against control values. Experiments and plots in **A–D** are representative of at least three independent experiments. In **E**, cells were treated with

0.5 mM paraquat, 2.5 mM MPP^+ or 4 μM rotenone for 48 h. Then, cells were co-stained with DHE (cytosolic ROS) or MitoSOX (mitochondrial ROS) and analyzed by FACS. Results are represented as the increase in DHE or MitoSOX mean fluorescence with respect to controls and are means ± SE of three replicas.

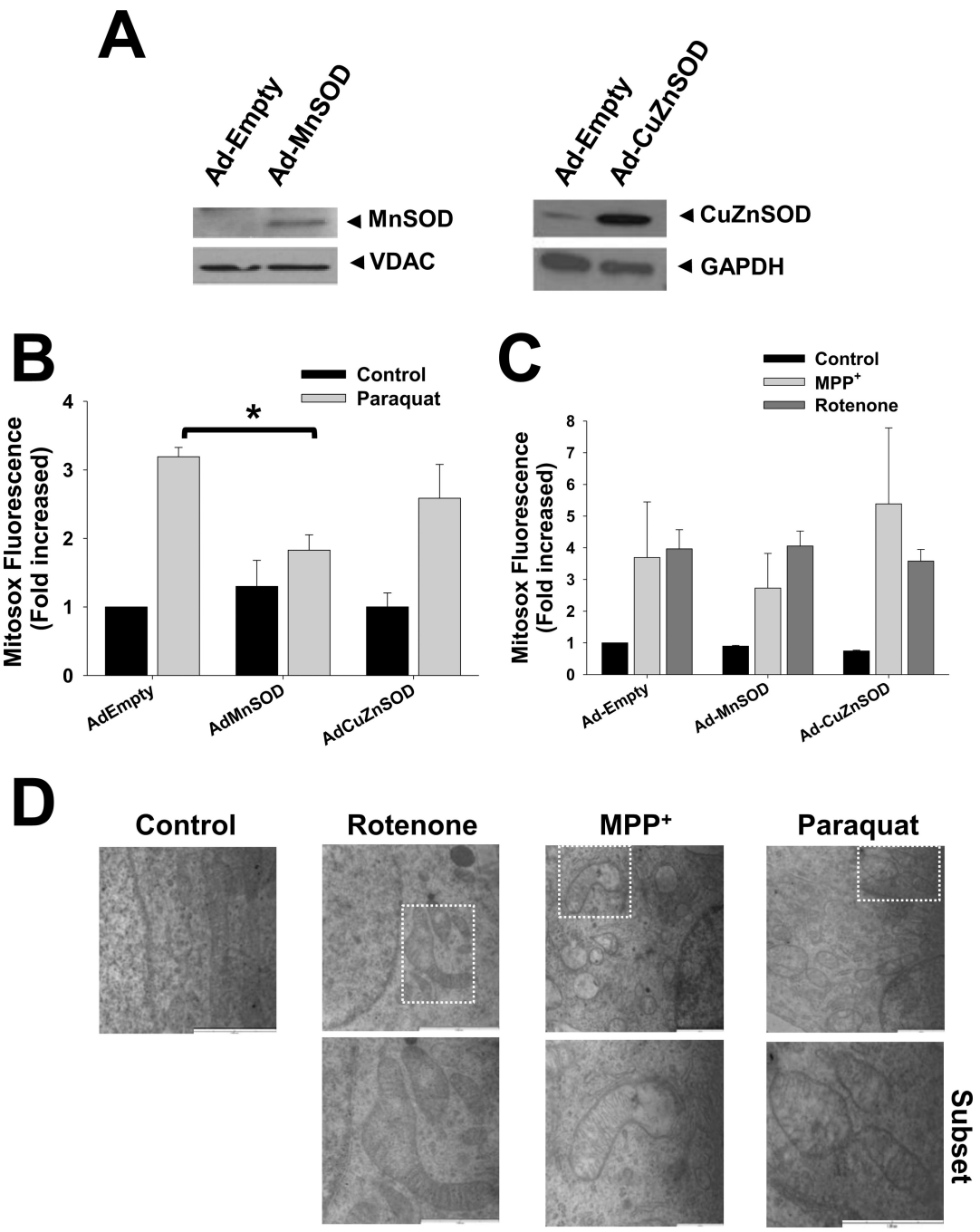

Figure 2. Mitochondrial damage and effect of SOD overexpression in ROS formation

Cells were transduced with Ad-MnSOD, Ad-CuZnSOD or Ad-Empty. In **A**, isolation of mitochondrial and cytosolic fractions was performed by differential centrifugation. Western blot analysis demonstrates the increased expression of SOD enzymes. VDAC and GAPDH signal was used as loading control for mitochondrial and cytosolic fractions respectively, and to evaluate cross-contamination of subcellular fraction (not shown). In **B–C**, cells transduced with viruses were treated with 0.5mM paraquat, 2.5 mM MPP^+ or 4 μM rotenone for 48 h. Mitochondrial $O_2^{\bullet -}$ was determined using MitoSOX as explained in Figure 1. In **D**,

cells were treated with parkinsonian toxins as explained above for 24 h and then, fixed with 2% glutaraldehyde. Fixed cells were processed for TEM. Blots (**A**), and images (**D**) are representative experiments and data in **B** and **C** are means ± SE of at least three independent replicas. *p<0.05 *vs* Ad-Empty + paraquat values.

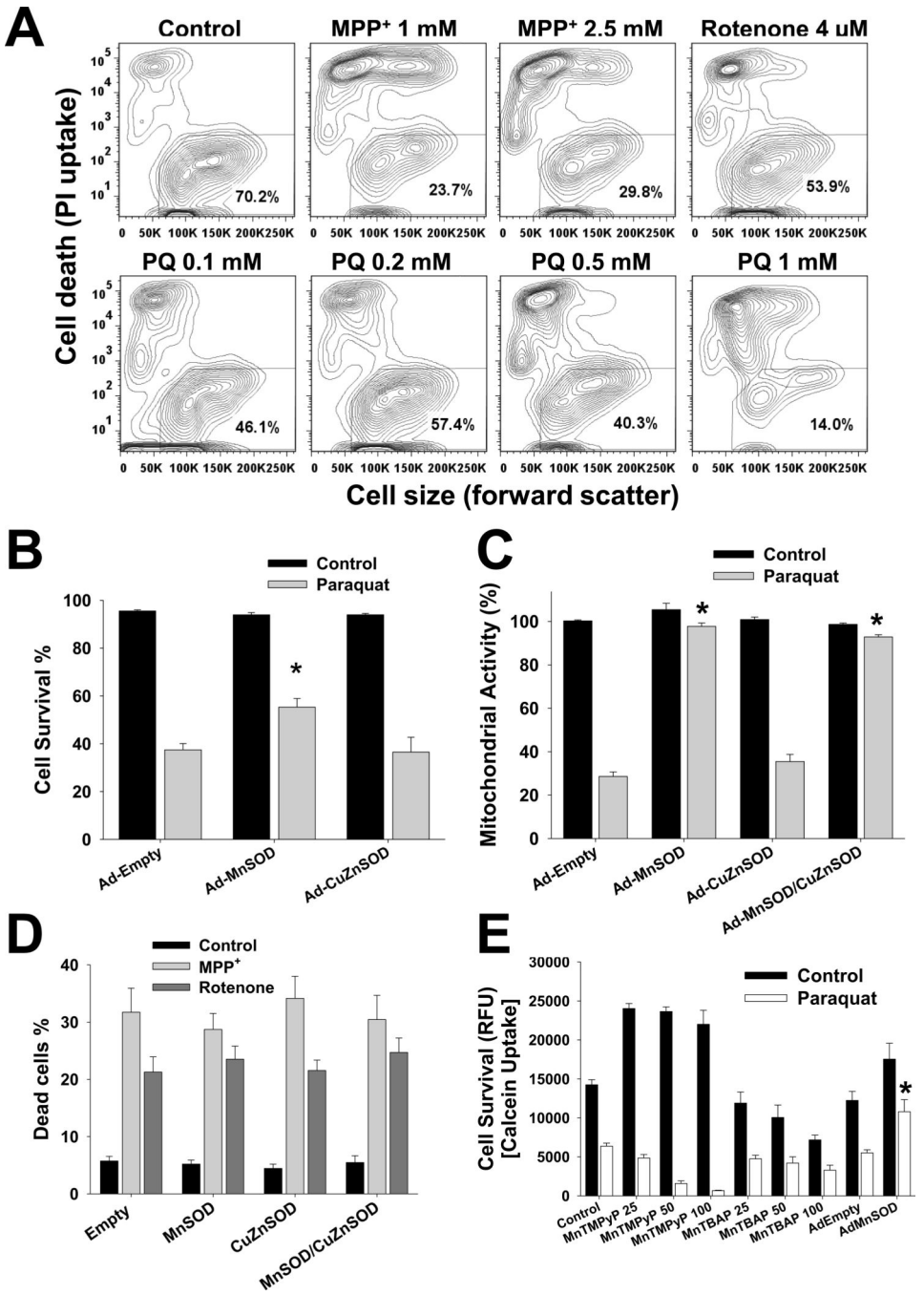

Figure 3. Effect of overexpression of SODs on dopaminergic cell death induced by parkinsonian toxins

In **A**, cells were treated with paraquat, MPP^+ or rotenone for 48 h and stained with PI. Cell death was analyzed in a forward scatter vs PI contour plot to depict cells with both a decrease in cell size (a marker for apoptosis) and loss of plasma membrane integrity. %s represent the population of cells with low PI and normal cell size (healthy cells) depicted in the lower right region. In **B–D**, cells were transduced with Empty, MnSOD or CuZnSOD adenoviruses 24 h prior exposure to parkinsonian toxins. Cell survival (**B**) or cell death (**D**)

was determined analyzing the % of cells with low or high PI staining, respectively. In **C**, alterations in mitochondrial activity were determined using the MTT assay. The effect of MnTBAP and MnTMPyP porphyrins on the survival of cells exposed to the parkinsonian mimetics was quantified by Calcein retention (**E**). Porphyrins were present throughout the experiment and concentrations used are indicated in μM. Data in **B–E** represent means ± SE of at least three replicas. *$p<0.05$ *vs* Ad-Empty + paraquat values.

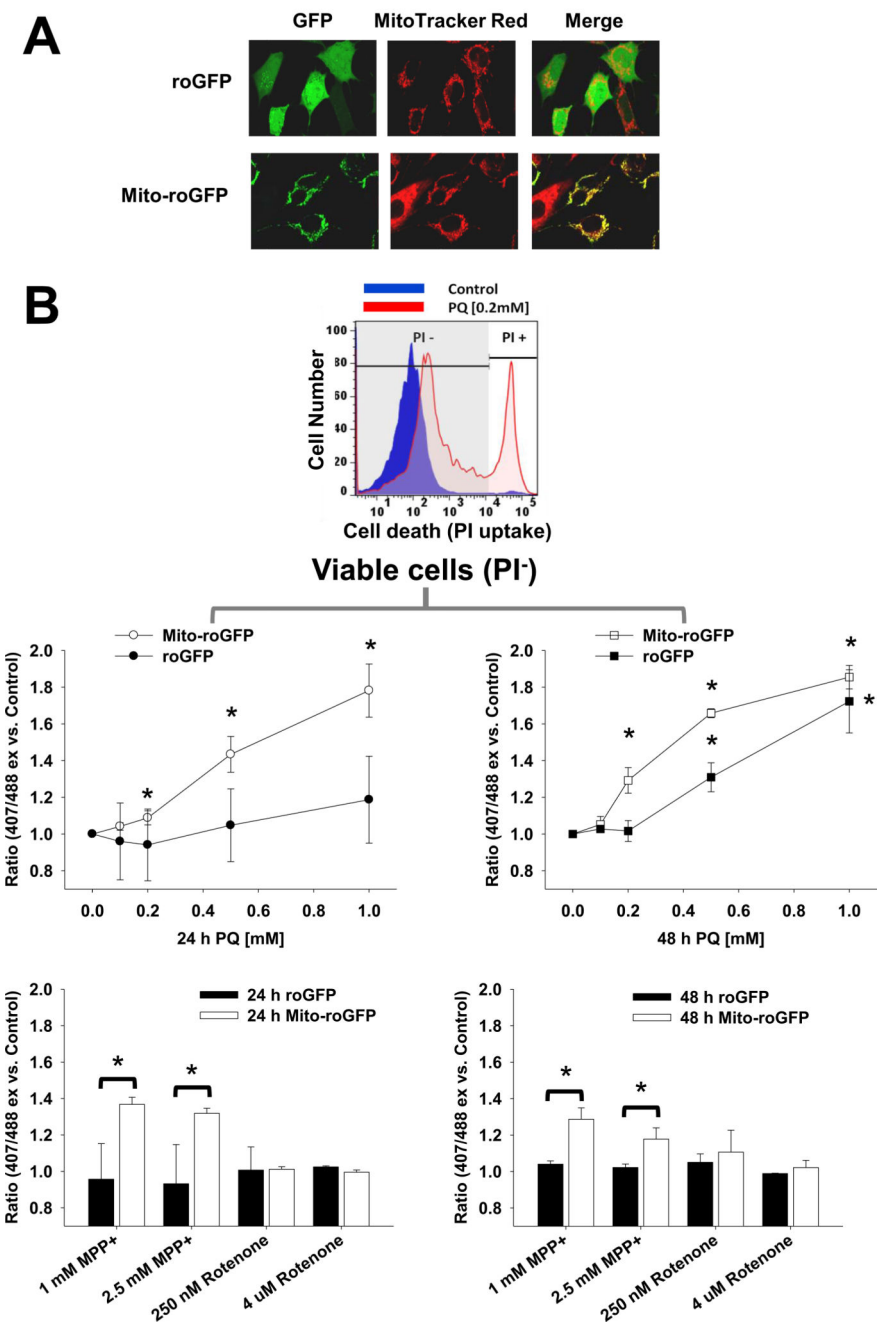

Figure 4. Alterations in the redox state of cytosol and mitochondrial compartments in response to parkinsonian neurotoxins

In **A**, stable cells overexpressing roGFP and Mito-roGFP were stained with MitoTracker Red to depict mitochondrial localization of Mito-roGFP. In **B**, roGFP and Mito-roGFP cells were treated with paraquat, MPP^+ or rotenone as indicated. Cells were co-stained with PI and only viable cells were analyzed (*see population of PI- cells in the grey region of the histogram*). Alterations in the redox state were determined by ratiometric analysis of changes in (Mito-)roGFP fluorescence at 407/488 ex and 530 em normalized with respect to

control values. Data in graphs represent means ± SE of at least five independent experiments. *p<0.05 *vs* control values.

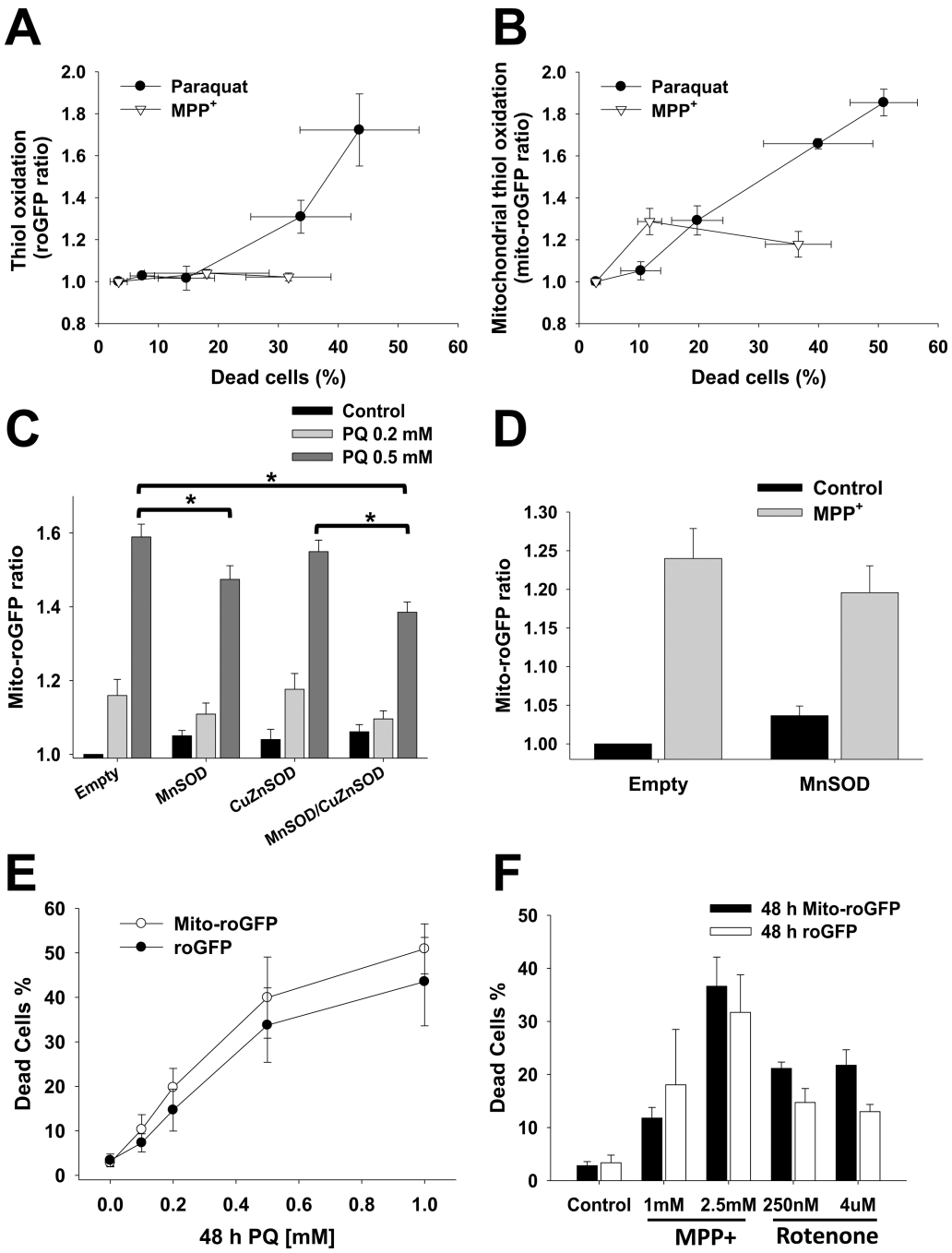

Figure 5. Relationship between cell death and alterations in the redox state of cytosol and mitochondria, and effect of SOD overexpression

In **A** and **B**, stable cells overexpressing roGFP and mito-roGFP were treated with 0.5 mM paraquat and 2.5 mM MPP^+ for 48 h. Cells were co-stained with PI and only viable cells (PI-) were analyzed for alterations in (Mito-)roGFP fluorescence as explained in Figure 4. Cell death was plotted against (Mito-)roGFP ratio to depict the relationship between cell loss and alterations in the redox balance of the cytosol and mitochondrial compartments. In **C** and **D**, cells were transduced with Empty, MnSOD or CuZnSOD adenoviruses and treated

24 h after infection. Alterations in Mito-roGFP fluorescence were determined as explained before. In **E** and **F**, stable cells overexpressing roGFP and Mito-roGFP were treated with paraquat, MPP^+ or rotenone as indicated. Cells were co-stained with PI and cell death was quantified as explained in Figure 3. Graphs represent means ± SE of at least five independent experiments. *$p<0.05$.

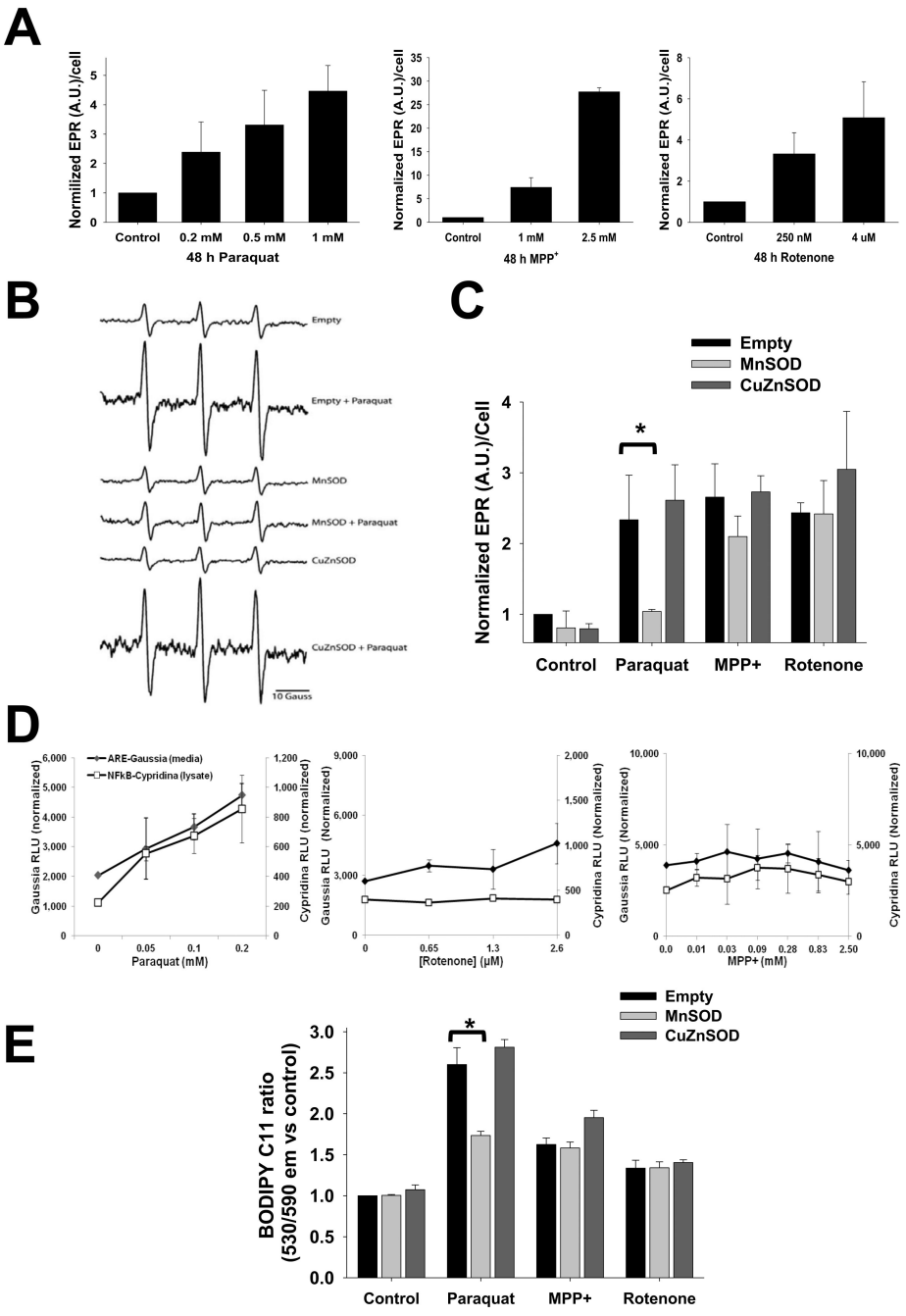

Figure 6. Determination of free radical formation, activation of ARE- and NF-κB-driven reporters, and lipid peroxidation induced by parkinsonian neurotoxins

In **A–C**, cells were treated with parkinsonian mimetics as depicted. Then, cells were loaded with the cell permeable spin probe CMH (200 μM, 60 min). After CMH incubation, cells were collected and EPR signal was detected in a Bruker e-scan EPR spectrometer. In **A** and **C**, EPR signal was normalized with the number of cells present after treatment and compared to control values. In **B** and **C**, cells were transduced with Empty, MnSOD or CuZnSOD adenoviruses and 24 h after infection, cells were treated with parkinsonian toxins

(0.5 mM paraquat, 2.5 mM MPP^+ or 4 uM rotenone) for 48 h. Data in **B** are representative EPR spectra from experiments in **C.** In **D**, human IMR-32 neuroblastoma cells were transfected with ARE-Gaussia, NF-κB-Cyrpidina, and CMV-Red Firefly reporter plasmids. 24 h after transfection, cells were treated for 5 h with paraquat, rotenone or MPP^+ at the concentrations indicated. Then, luciferase activity was assessed in media (ARE) and lysate (NF-κB). Results are normalized by Red Firefly activity and expressed as RLUs. In **E**, lipid peroxidation was determined using the ratiometric probe BODIPY C11, whose emission fluorescence at 590 nm decreases with a concomitant in the fluorescent spectra at 530 nm in response to oxidation. Cells were treated as explained in **C** and incubated for 30 min prior to FACS analysis with BODIPY C11 (2.5 μM). Results were analyzed ratiometrically 530/590 em normalized with control values. Graphs represent means ± SE of at least 5 independent experiments. *$p<0.05$ *vs* Ad-Empty values.

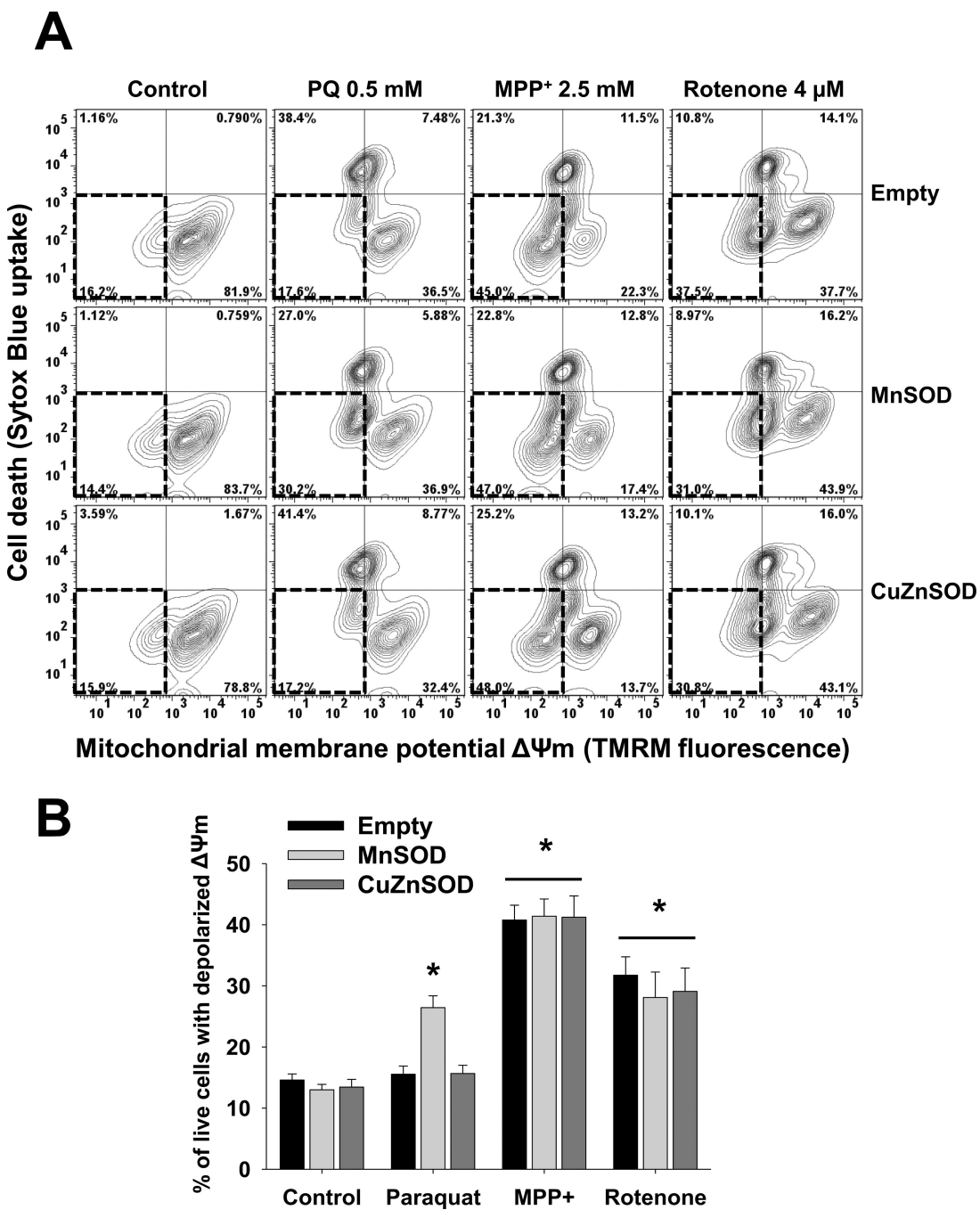

FIGURE 7. MnSOD overexpression decreases cell death but mitochondrial membrane potential (ΔΨm) loss induced by paraquat

Cells were transduced with Empty adenovirus or adenovirus encoding MnSOD or CuZnSOD for 24 h prior exposure to parkinsonian toxins. In **A**, cells were treated with paraquat, MPP^+ or rotenone for 48 h and stained with TMRM (50 nM) and Sytox Blue (5 nM) 15 min prior FACS analysis. Loss of ΔΨm and cell death were simultaneously analyzed in a TMRM *vs* Sytox Blue contour plot to depict cells with a decrease in ΔΨm (TMRM fluorescence, *left quadrants*) and loss of plasma membrane integrity (increased Sytox Blue

uptake, *upper quadrants*). In **B,** % of cells with low Sytox Blue fluorescence and reduced TMRM signal depict live cells with ΔΨm depolarization (*from broken line-lower left quadrants in* **A**). Data in **B** represent means ± SE of at least three replicas. *p<0.05 *vs* Ad-Empty in the absence of treatment.